

Reactions between Li Atoms and HX (X = F, Cl) Molecules: Semiempirical SCF MO and Matrix Isolation ESR Studies

Paul H. Kasai

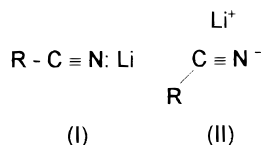
IBM Research Division, Almaden Research Center, 650 Harry Road, San Jose, California 95120-6099

Received: November 23, 1999; In Final Form: February 14, 2000

Examination of reaction between the Li atom and the HX (X = F, Cl) molecule by a semiempirical molecular orbital method (AM1) revealed the spontaneous formation of the Li:HCl and Li:HF complexes with the respective heats of complexation of 75 and 84 kJ/mol. The calculations yielded totally different structures for the two complexes, however. In the Li:HCl complex, the unpaired electron is in the antibonding σ orbital of the H–Cl moiety and the elongated H–Cl is sided by the Li atom bearing a substantial positive charge (+0.47). For the Li:HF complex, a linear Li–F–H structure was predicted. The unpaired electron resides in a s–p hybridized orbital of the Li atom directed away from the F atom, and the complex is formed by the dative interaction of the fluorine electrons with vacant Li orbitals. A substantial net negative charge (–0.18) is thus borne by the Li atom of the complex. Examination by ESR of argon matrixes in which Li atoms and HCl (and HF) molecules had been co-condensed indeed revealed the spontaneous formation of complexes exhibiting the ESR spectra which were in total accord with the structures and the SOMOs (singly occupied molecular orbitals) predicted above. In the case of Li/HCl/Ar system, the formation of the second complex, Li₂Cl, was observed and was ascribed to the reaction between Li atoms and LiCl molecules inadvertently formed during deposition (Li + HCl → H + LiCl). An examination of the Li:LiCl system by the AM1 method revealed a spontaneous formation of the complex with the heat of complexation of 121 kJ/mol. The complex has an isosceles triangular form, and the unpaired electron renders a bent, one-electron bond between the two Li atoms.

Introduction

Recently we examined the (possible) reactions between Li atoms and RCN (R = H, CH₃) molecules by a semiempirical SCF molecular orbital method (MNDO) and by matrix isolation ESR spectroscopy.¹ The theory predicted the formation of a linear complex **I** if the Li atom approached the RCN (R = H, CH₃) molecule from the nitrogen end, and a side-on complex **II** if the Li atom approached the RCN molecule from the broad side.



In either case the reaction proceeds spontaneously. It is driven by the attainment of a *three electron bonding system*, two electrons being in the orbital given by the symmetric combination of the Li 2s valence orbital and the nitrogen lone pair orbital in the former case, and the bonding p_π orbital in the latter, and the third electron being in the orbital given by their antisymmetric combination. The ESR study of argon matrixes in which these reacting species had been co-condensed at near liquid helium temperature clearly revealed the spontaneous formation of two complexes with the spectral patterns in total accord with the structures and SOMOs (singly occupied molecular orbitals) predicted by the theory.

Lindsay et al. reported earlier on the ESR spectra of Na:HCl and K:HCl complexes generated in argon matrixes.^{2,3} The

complexes were observed when the alkali metal atoms and HCl molecules were co-condensed in argon matrixes. The reaction was postulated to be an electron jump process (e.g., K + HCl → K⁺ + HCl[–]) followed by stabilization of the otherwise unstable HCl anion by the cation. The unpaired electron was found in the antibonding σ orbital of the HCl moiety. No hfs (hyperfine structure) due to the alkali nucleus was observed, however, and the structure of the complexes was not discussed. In the case of the Na/HCl/Ar system, the Na:HCl complex was observed only after prolonged irradiation of the matrix by a xenon arc light. A photoassisted process was hence suggested for its formation.³

It seemed that the reaction between an alkali metal atom and an HX molecule ought to proceed spontaneously driven initially by a three electron bonding scheme similar to that invoked above for the Li/RCN system. We therefore examined the (possible) reaction process between the Li atom and the HCl molecule and that between the Li atom and the HF molecule first by the semiempirical SCF molecular orbital method (AM1),⁴ and then experimentally by matrix isolation ESR spectroscopy. The theoretical study predicted the spontaneous formation of Li:HCl and Li:HF complexes both driven by the three electron bonding scheme but leading to totally different structures. The ESR study revealed the formation of the complexes with the spectral patterns which were in excellent accord with the structures and the SOMOs predicted by the theory. In the case of Li/HCl/Ar system, the formation of the second complex, Li₂Cl, was observed and was ascribed to the reaction between the Li atom and the LiCl molecule driven, here again, by the three electron bonding scheme.

Experimental and Computational Technique

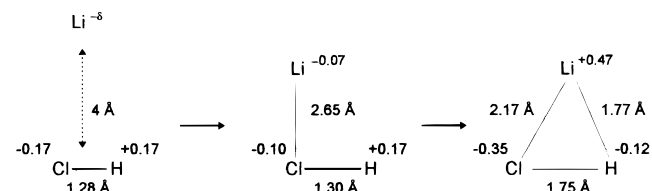
A liquid helium cryostat that would allow trapping of vaporized metal atoms in an argon matrix and examination of the resulting matrix by ESR has been described earlier.^{5,6} In the present series of experiments, Li atoms were vaporized from a resistively heated (~ 550 °C) stainless steel tube and were trapped in argon matrixes containing HCl or HF molecules (1%). All the ESR spectra were obtained while the matrix was maintained at ~ 4 K. The spectrometer frequency locked to the sample cavity was 9.425 GHz. For photoirradiation of the matrix, a high-pressure Xe–Hg lamp (Oriel, 1 kW unit) was used. The light beam was passed through a water filter, followed by a broad band interference filter of choice, and was focused on the coldfinger ~ 40 cm away.

Both HCl and HF (in a lecture bottle) were obtained from Matheson Gas Products and used as received. Li metal was obtained from Alfa Products, and ^6Li metal (enrichment $>95\%$) was obtained from U.S. Services, Inc.

For examination of the viable reaction passages by the semiempirical SCF molecular orbital method, the AM1 program implemented in HyperChem was used.⁷ In each case the HX ($X = \text{Cl}$ or F) molecule was first geometry optimized and the reacting metal atom, Li, was placed ~ 4 Å away; the total system was then geometry optimized following the energy surface trough (the steepest descent).

Results

SCF Semiempirical Molecular Orbital Study. Geometry optimization of a reacting system consisting of the Li atom and the HCl molecule ~ 4 Å apart by the AM1 semiempirical SCF molecular orbital method, independent of the initial position of the Li atom relative to the HCl molecule, consistently delineated the reaction passage that would attain and increase the overlap between the Li 2s valence orbital and the Cl p_π orbital. The Li atom thus eventually assumed the position ~ 2.7 Å away from the Cl atom with the Li–Cl internuclear direction perpendicular to the Cl–H bond. At this point the unpaired electron is in a Li sp hybridized orbital directed away from the Cl atom, and the Li atom bears a negative charge of ~ 0.07 owing to the Cl p_π electrons datively interacting with the vacant Li orbital. From here on, as the Li atom moved toward the broad side of the HCl moiety, a rapid charge transfer occurred as the unpaired electron migrated into the HCl antibonding σ orbital, and the final structure was attained as depicted below.



The initial half of the reaction is driven solely by the three electron bonding scheme where the pair of the Cl p_π electrons go into the orbital given by the bonding combination of the Cl p_π orbital and the Li 2s valence orbital, and the third electron goes into the orbital given by their antibonding combination. When the energy level of the antibonding combination crosses the level of the antibonding σ orbital of the HCl sector, the unpaired electron migrates into the antibonding σ orbital. Figure 1 illustrates the isosurface contours of the orbitals involved in the three electron bonding scheme just at the onset of the charge transfer, and those of the orbital of the bonding combination and the SOMO of the final adduct radical. As revealed there,

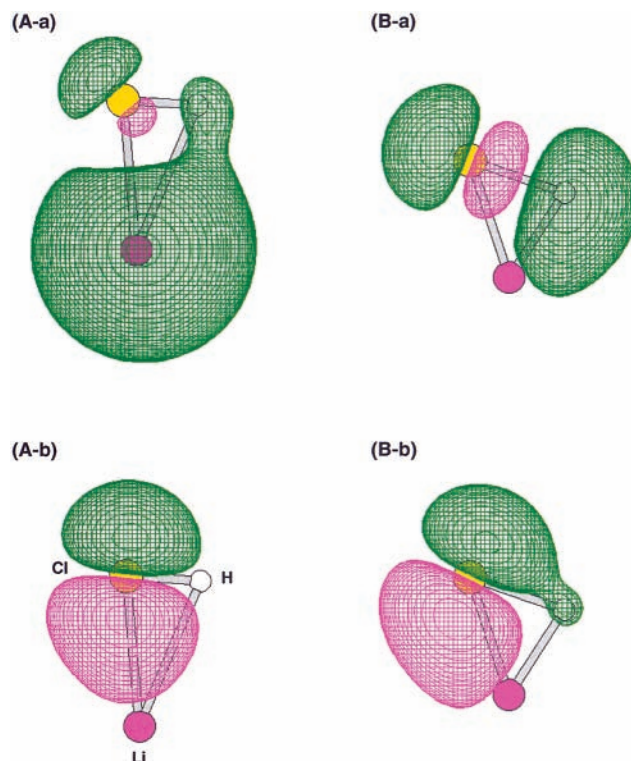
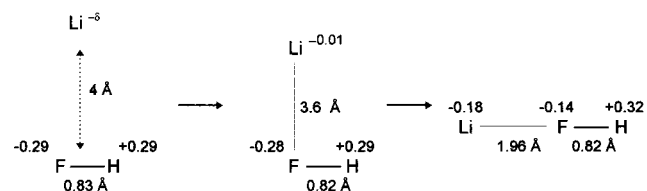


Figure 1. Isosurface contours of the orbitals given by the antibonding and the bonding combination of the valence orbital of the approaching Li atom and the chlorine p_π orbital of HCl: (A-a) and (A-b) at the onset of unpaired electron migration; (B-a) and (B-b) in the final adduct radical.

the migration of the unpaired electron from the Li 2s orbital into the H–Cl antibonding σ orbital is nearly complete. The charge on the Li atom is partially compensated by the Cl p_π electrons datively donated in the orbital of the bonding combination.

A similar computation performed for the Li atom and the HF molecule placed ~ 4 Å apart revealed the following reaction passage.



When the Li atom was placed ~ 4 Å away on the broad side of the HF molecule, the initial process was driven by the three electron bonding scheme involving the F p_π orbital and the Li 2s orbital (as in the case of the Li atom and the HCl molecule), but when the Li atom reached the position above the F atom, the three electron bonding scheme involving the F p_σ orbital became more dominant, and the Li atom moved to attain the final linear structure as shown. If the Li atom was placed initially on the left side of the F atom (in the depiction given above), the reaction was driven by the latter three electron bonding scheme throughout. Thus most intriguingly no migration of the unpaired electron occurs in the Li/HF system. Figure 2 shows the isosurface contours of the F p_σ orbital datively interacting with the Li valence orbital and the SOMO of the final adduct radical.

Because of the prominent role played in the crossed molecular beam experiment, many theoretical studies of the reaction path

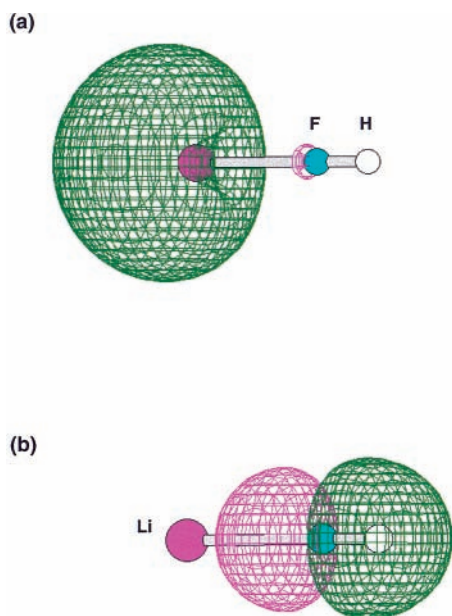
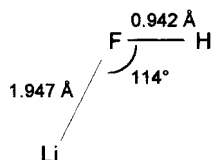


Figure 2. Isosurface contours of orbitals of the Li:HF complex: (a) orbital given by the antibonding combination of the Li valence orbital and the F p_{σ} orbital and (b) orbital given by their bonding combination.

surface energy of the reaction $\text{Li} + \text{HF} \rightarrow \text{LiF} + \text{H}$ have been performed using various methods at varying degrees of sophistication.⁸ The ab initio study by Chen and Schaefer, for example, revealed the formation of the Li:FH complex of a bent form when the reaction proceeded following the minimum energy pathway.^{8a}



When the Li atom approached the F atom collinearly, an energy minimum was located at $r_{\text{Li-F}} \cong 2.0$ Å and this saddle point was only ~ 2 kcal above the global minimum of the bent complex. It is shown that the potential energy curve of the complex as the function of the Li-F-H angle is shallow and rather flat in the 90° – 180° range.^{8a}

The AM1 calculations yielded the LCAO descriptions of the SOMO of the side-on Li:HCl complex and that of the end-on Li:HF complex as shown below.

$$\Phi_{\text{SOMO}}(\text{Li:HCl}) = a\text{H}(1s) - b\text{Cl}(2p_z) - c\text{Li}(2s) \quad (1)$$

where $a^2 = 0.59$, $b^2 = 0.36$, and $c^2 = 0.03$.

$$\Phi_{\text{SOMO}}(\text{Li:HF}) = a\text{Li}(2s) + b\text{Li}(2p_z) \quad (2)$$

where $a^2 = 0.92$ and $b^2 = 0.07$.

The AM1 calculation performed for the Li:HF complex of the bent form given by the ab initio calculation yielded the SOMO essentially identical to that of the linear structure. It is thus predicted that the ESR spectral pattern of the Li:HCl complex is predominantly determined by a large, essentially isotropic hfc (hyperfine coupling) tensor of the hydrogen nucleus, while that of the Li:HF complex is predominantly determined by a large, essentially isotropic hfc tensor of the Li nucleus.

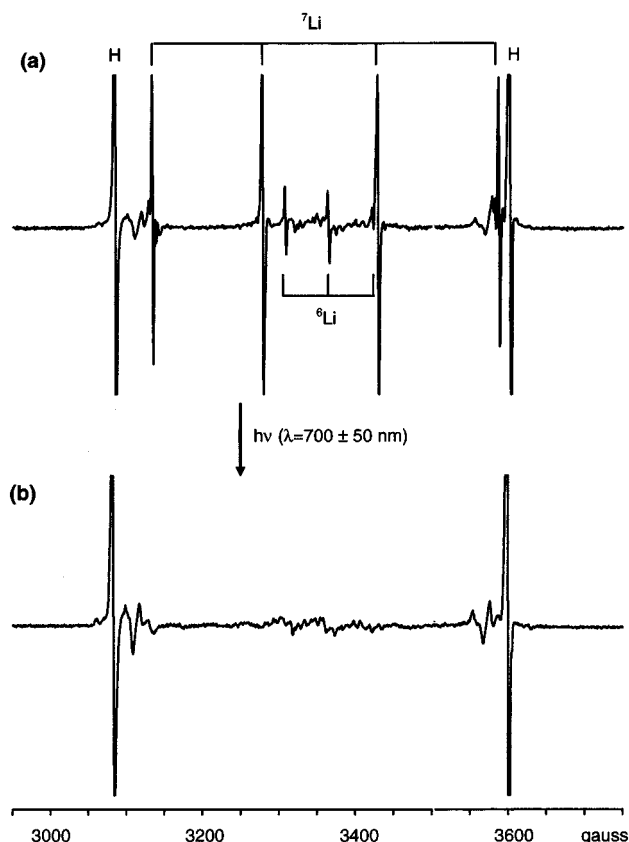


Figure 3. ESR spectra observed from the Li/HCl(1%)/Ar system: (a) prior to and (b) after irradiation with red light ($\lambda = 700 \pm 50$ nm) for 10 min.

Matrix Isolation ESR Studies. Li/HCl/Ar System. Figure 3a shows the ESR spectrum of an argon matrix in which Li atoms and HCl molecules had been co-condensed. The quartet due to isolated ^7Li atoms ($I = 3/2$, natural abundance = 92.6%, and $\mu = 3.256 \beta_n$), the triplet due to isolated ^6Li atoms ($I = 1$, natural abundance = 7.4%, and $\mu = 0.822 \beta_n$), and the doublet due to isolated hydrogen atoms were readily recognized as indicated. Weak additional groups of signals are noted near the hydrogen doublet and also between the inner components of the ^7Li quartet. The presence of isolated hydrogen atoms is attributed to a (thermally excited) process that occurs when Li atoms and HCl molecules collide above the cold finger during the matrix deposition.

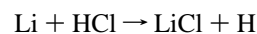


Figure 3b shows the spectrum observed from the same matrix after it had been irradiated with red light ($\lambda = 700 \pm 50$ nm) for 10 min. The irradiation resulted in the total disappearance of the signals due to isolated Li atoms and a severalfold increase in the intensity of the hydrogen doublet. The technique of co-condensing metal atoms of low ionization potential and molecules with some electron affinity in an argon matrix and effecting electron transfer between them by mild radiation, thus generating *chemically isolated* metal cations and molecular anions, had been demonstrated some time ago.⁵ When the acceptor molecules are of the form HX (where X is a strong electrophile), the dissociative electron capture, $\text{HX} + e^- \rightarrow \text{H}\bullet + \text{X}^-$, often occurs spontaneously. The observed photoinduced spectral change is thus attributed to the following reaction.



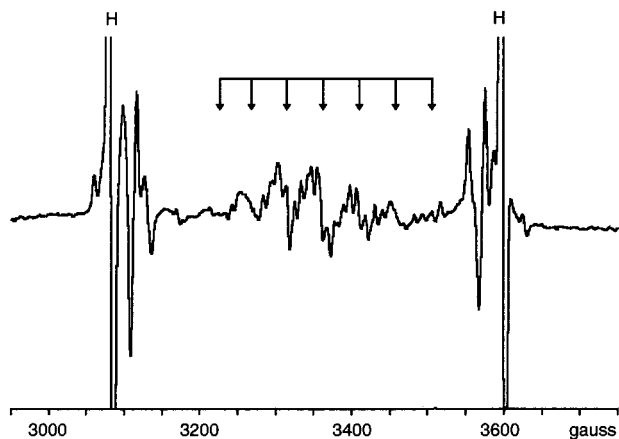


Figure 4. ESR spectrum of the ${}^7\text{Li}/\text{HCl}(1\%)/\text{Ar}$ system observed after photoirradiation ($\lambda = 700 \pm 50$ nm) for 10 min. Figure 3b is shown with a higher vertical gain. The septet-of-quartet pattern is recognized as indicated and is assigned to the Li:LiCl complex.

The $2s \rightarrow 2p$ transition of the Li atom occurs at $\lambda = 670$ nm. It should be noted that the electron transfer stipulated here occurs between Li atoms and HCl molecules that are separated. The groups of weak signals near the hydrogen doublet and also those initially noted between the inner components of the ${}^7\text{Li}$ quartet are now observed with less or little interference from other signals. The photoirradiation with red light had little effect on those signals. Figure 4 shows the spectrum observed after the photoirradiation with a higher vertical magnification. The groups of signals in the central sector are thus recognized as a septet of quartet as indicated.

Based on the theoretical result presented in the preceding section, the groups of signals near the hydrogen doublet were assigned to the Li:HCl complex formed spontaneously between Li atoms and HCl molecules trapped nearby. The hydrogen hfc tensor of the complex is thus only slightly smaller than that of isolated hydrogen atoms. As for the source of the signals in the central sector, the essentially isotropic septet pattern strongly indicates a radical species involving two equivalent Li nuclei; the minor quartet pattern is then attributed to a Cl nucleus. The septet-of-quartet pattern was hence assigned to a complex formed spontaneously between Li atoms and LiCl molecules which had been generated in the vapor phase process discussed above and trapped nearby.

Figure 5 shows the corresponding spectra obtained when the experiment was repeated using ${}^6\text{Li}$ atoms (enrichment $>95\%$). The isotopic substitution had little effect on the overall pattern of the spectrum assigned to the Li:HCl complex, though some components appeared sharper. The signals assigned to the Li:LiCl complex showed an expected profound isotopic substitution effect.

The spectral patterns due to the Li:HCl complex observed from the ${}^7\text{Li}/\text{HCl}/\text{Ar}$ and the ${}^6\text{Li}/\text{HCl}/\text{Ar}$ systems are shown in an expanded scale in Figure 6a,b. Thus, for the ESR spectrum of the Li:HCl complex, the finer structural features revealed in each component of the doublet (due to the hydrogen nucleus) were analyzed and assigned to an axially symmetric hfc tensor of the Cl nucleus as indicated. Though no hyperfine structures due to the Li nucleus are resolved, it is clearly revealed that many structural features appear sharper in the spectrum observed from the ${}^6\text{Li}/\text{HCl}/\text{Ar}$ system. Based on the indicated analysis, the \mathbf{g} tensor, the proton hfc tensor, and the ${}^{35}\text{Cl}$ hfc tensor of the Li:HCl complex were determined as given in Table 1. A computer program that simulates an ESR spectrum given by an ensemble of randomly oriented radicals has been described

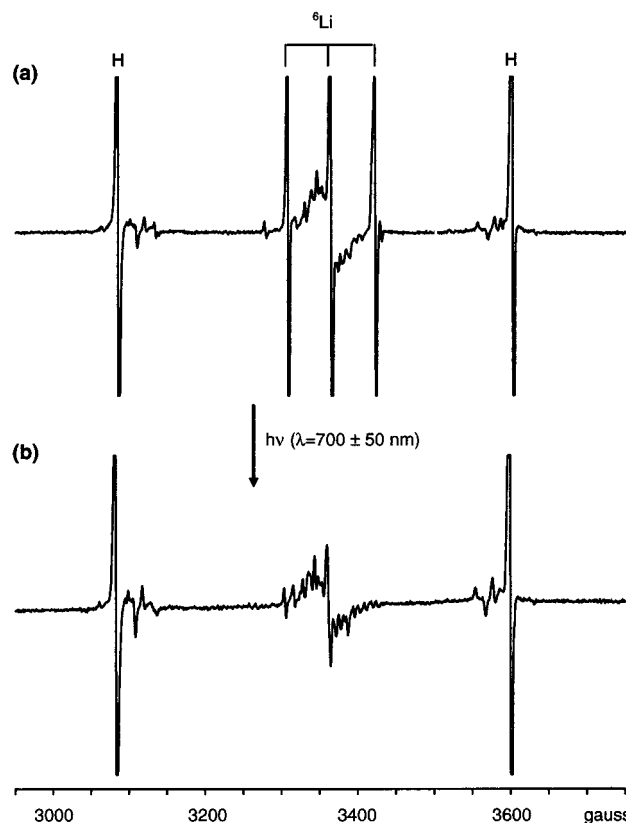


Figure 5. ESR spectra observed from the ${}^6\text{Li}/\text{HCl}(1\%)/\text{Ar}$ system: (a) prior to and (b) after irradiation with red light ($\lambda = 700 \pm 50$ nm) for 10 min.

earlier.⁹ The effect of the orientation of a hyperfine coupling tensor not being collinear with that of the \mathbf{g} tensor is addressed in terms of the Eulerian angles relating the orientations of the two tensors. Figure 6c shows the computer simulated spectrum based on the \mathbf{g} tensor and the proton and chlorine hfc tensors of the Li:HCl complex given in Table 1. A Lorentzian line shape with the line width of 2 G (a half-width at half-height) was assumed for the simulation, and the signals due to isolated hydrogen atoms were superposed for direct comparison.

Efforts to obtain a spectrum of the Li:LiCl complex with a higher signal-to-noise ratio (hence of improved resolution) by changing the relative and/or absolute concentrations of the reactants, Li atoms, and HCl molecules, were not fruitful. From the spectrum shown in Figure 4 the \mathbf{g} tensor and the isotropic components of the ${}^7\text{Li}$ and ${}^{35}\text{Cl}$ hfc tensors were assessed as given in Table 1. A closer inspection of the septet pattern reveals, however, that the chlorine hyperfine structures are less well-resolved in the even-number components indicating the presence of an alternating line width effect. The effect could be accounted for by some anisotropy of the lithium hfc tensor as shown later in the discussion section.

Li/HF/Ar System. Parts a and b of Figure 7 show, respectively, the ESR spectra observed from the Li/HF(1%)/Ar system prior to and after photoirradiation with red light ($\lambda = 700 \pm 50$ nm) for 10 min. It is immediately apparent that the system is devoid of a complex showing a proton hfc interaction close to that of isolated hydrogen atoms (as in the case of the Li/HCl/Ar system). The indicated quartet pattern (due obviously to a hfc interaction with a Li nucleus) was assigned to the Li:HF complex of a linear form predicted by the AM1 calculation. No hyperfine structures attributable to the fluorine nucleus were observed. The \mathbf{g} tensor and the ${}^7\text{Li}$ hfc tensor of the complex

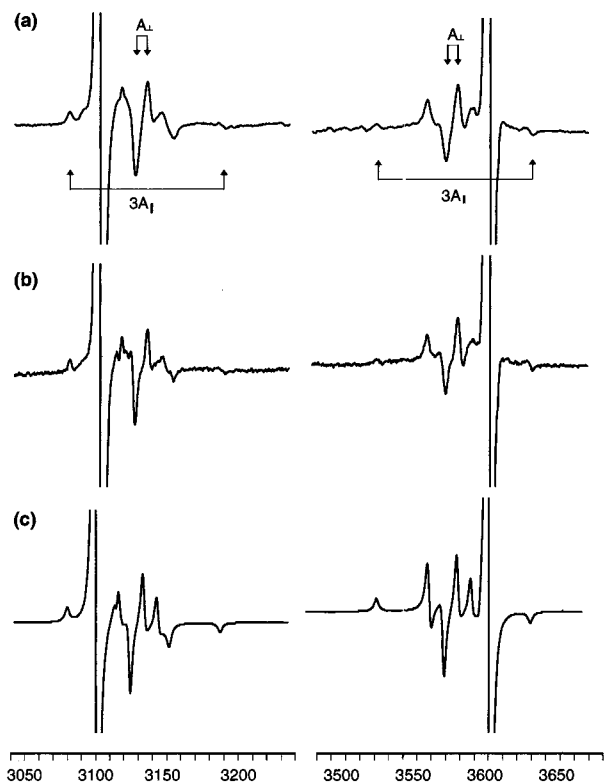


Figure 6. ESR spectral patterns due to the Li:HCl complex observed from (a) the $^7\text{Li}/\text{HCl}/\text{Ar}$ system, (b) the $^6\text{Li}/\text{HCl}/\text{Ar}$ system, and (c) simulated based on the g and the proton and chlorine hfc tensors given in Table 1. In (c) the signals due to isolated hydrogen atoms are superposed.

TABLE 1: g Tensors and Hyperfine Coupling Tensors (Gauss) Determined for Complexes Observed in the Alkali Metal/HCl (or HF)/Argon System

complex	g tensor	$A(\text{H})$	$A(^7\text{Li})$	$A(^{35}\text{Cl})$
	\parallel/\perp	\parallel/\perp	\parallel/\perp	\parallel/\perp
Li:HCl	2.0015/2.0035	445/448		37.3/10.0
Na:HCl ^a	2.0008	417.0		40.2
K:HCl ^b	2.0017/2.0031	427.3/430.0		47.3/19.0
Li:LiCl	2.002		47/49/45 ^c	10.0
Li:HF	1.9987		90/96	
H atom ^c	2.00179	504.85		
Li atom ^{c,d}	2.00038		148.6	
	2.00123		142.6	

^a From ref 1. ^b From ref 2. ^c The values determined presently for atoms isolated in argon matrices. ^d There are two major trapping sites for Li atoms in argon matrices. ^e The orientations of the two Li hfc tensors differ within the molecular plane by $\pm 45^\circ$.

determined from the spectrum are given in Table 1. Figure 7c shows the computer simulated spectrum based on these tensors. The experiment repeated using ^6Li metal showed the expected isotope substitution effect.

Discussion and Summary

Shown in Figure 8 are the energy levels of the halogen p_π orbital and the antibonding σ orbital of the H-X (X = F, Cl) molecule given by the AM1 method. Also shown between the dotted lines is the energy level of the Li 2s orbital. The figure readily offers an explanation why, as the three electron bonding scheme advances between the Li valence electron and the halogen p_π electrons, the migration of the unpaired electron into the antibonding σ orbital of the H-X moiety would occur for HCl but not for HF.

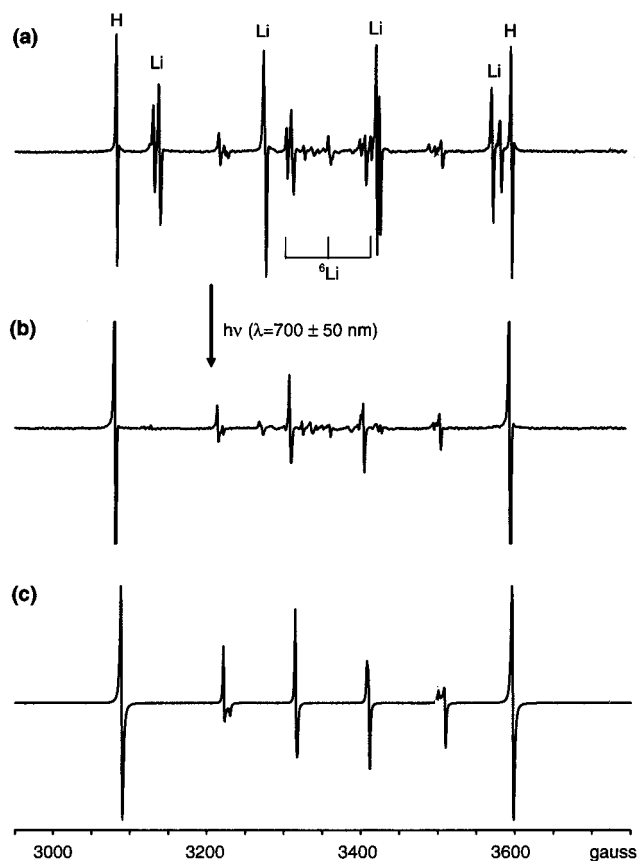


Figure 7. ESR spectra observed from the Li:HF(1%)/Ar system: (a) prior to and (b) after irradiation with red light ($\lambda = 700 \pm 50$ nm) for 10 min. (c) Spectrum of the Li:HF complex simulated based on the g tensor and the Li hfc tensor given in Table 1 (with the signals due to isolated hydrogen atoms superposed).

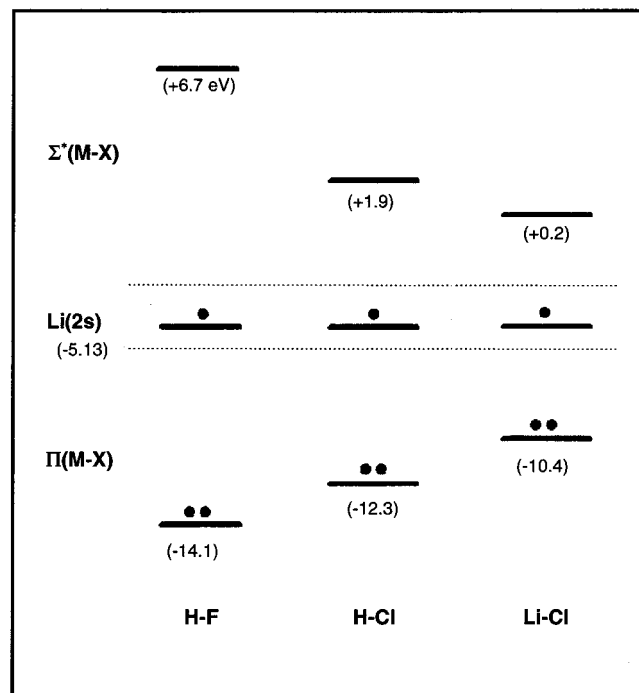


Figure 8. Energy levels of the halogen p_π orbitals and the antibonding σ orbitals of the HCl, HF, and LiCl molecules given by the AM1 method. The energy level of the Li 2s orbital is also indicated.

Also included in Figure 8 are the corresponding orbital levels for the Li:LiCl complexation process. It is thus expected that

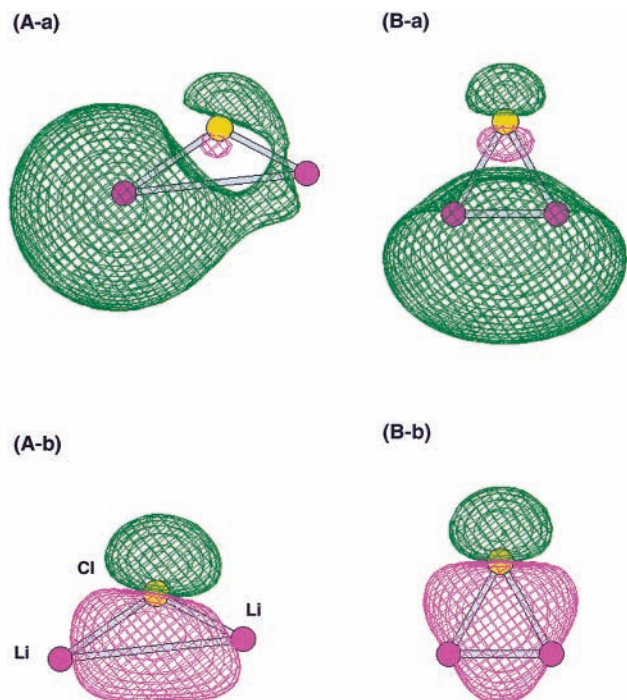
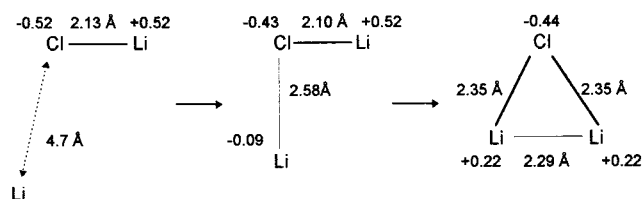


Figure 9. Isosurface contours of the orbitals given by the antibonding and the bonding combinations of the valence orbital of the approaching Li atom and the chlorine p_π orbital of LiCl: (A-a) and (A-b) at the onset of unpaired electron migration; (B-a) and (B-b) in the final adduct radical.

the process would be spontaneously driven initially by the three electron bonding scheme, and would be followed by migration of the unpaired electron into the antibonding σ orbital of the original Li-Cl sector. A typical reaction passage of the Li:LiCl complexation process given by the AM1 method is shown below. The calculation yielded the heat of complexation of 121



kJ/mol. The final complex thus has an almost-equilateral triangular form. Figure 9 illustrates the isosurface contours of the orbitals involved in the three electron bonding scheme just at the onset of the charge transfer and those of the orbital of the bonding combination and the SOMO of the final complex. It is thus revealed that, in the final complex, the unpaired electron renders a one electron bond between the two Li atoms. The bond is bent outward. The complex is held by the electrons in the bonding combination of the Cl p_π orbital and the Li valence orbitals.

The AM1 calculation yielded the LCAO description of the SOMO of the Li:LiCl complex as shown below.

$$\Phi_{\text{SOMO}}(\text{Li:LiCl}) = a[\text{Li}(2s) + \text{Li}'(2s)] + b[\text{Li}(2p_x) - \text{Li}'(2p_x)] - c[\text{Li}(2p_y) + \text{Li}'(2p_y)] + d\text{Cl}(2p_y) \quad (3)$$

where $a^2 = 0.35$, $b^2 = 0.03$, $c^2 = 0.09$, and $d^2 = 0.07$.

The ESR spectral pattern of the complex is thus predicted to be predominantly determined by the essentially isotropic hfc tensors of the two Li nuclei as observed.

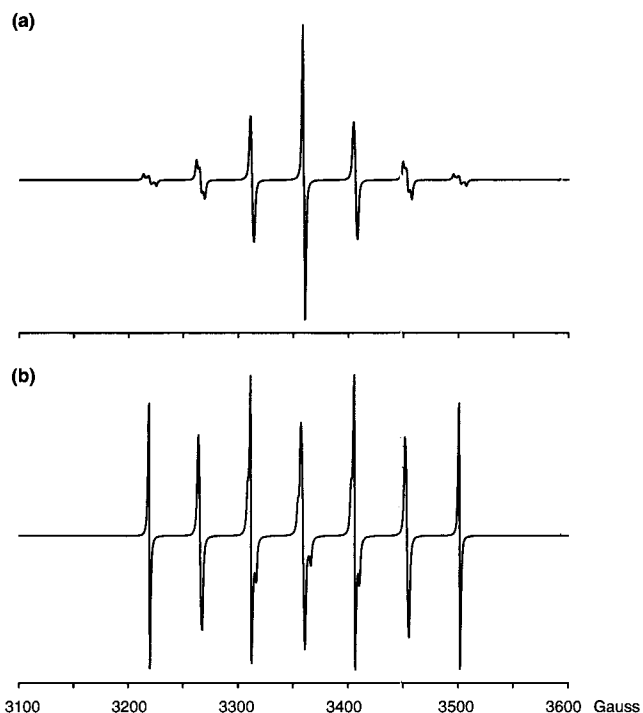


Figure 10. Septet patterns expected from the hfc interaction with two equivalent Li nuclei ($I = 3/1$) with the principal coupling elements of 45, 47, and 49 G: (a) the orientations of the two hfc tensors are coincident; (b) the each tensor is rotated about the axis of the intermediate element by $\pm 45^\circ$.

The hfc tensor of a magnetic nucleus consists of an isotropic component A_{iso} , and an orientation-dependent component A_{dip} . A general expression representing each element of the tensor A_{dip} may be given as

$$A_{ij}(=x,y,z) = g_e \beta_e g_n \beta_n \left\langle \Phi \left| \frac{3ij - \delta_{ij}r^2}{r^5} \right| \Phi \right\rangle$$

where r is the distance between the unpaired electron and the nucleus. Evaluation of the above expression by the wave function (3) using the Slater atomic orbitals revealed that (1) the principal (diagonal) hfc tensor of each Li nucleus would have the largest and the smallest elements in the molecular plane and the intermediate element in the direction perpendicular to the molecular plane, (2) the magnitude of the anisotropy would be ± 2 G, and (3) the direction of the largest hfc element of each Li tensor is rotated $\pm 45^\circ$ away from the Li-Li internuclear axis.¹⁰ As shown earlier, the Li hfc tensor of the Li:LiCl complex has been found to be essentially isotropic and is ~ 47 G. Figure 10a shows the computer-simulated septet pattern expected from the hfc interaction of two equivalent ^7Li nuclei with the principal coupling elements of 45, 47, and 49 G, respectively. Here it is assumed that the orientations of the two tensors are coincident. Shown in Figure 10b is the simulated spectrum using the same set of tensors but assuming that each tensor is rotated about the axis of the intermediate element by $\pm 45^\circ$. It is clearly shown that the "alternating line width effect" observed in the spectrum of the Li:LiCl complex (Figure 4) could be accounted for by the differing orientation of the Li tensors.

Included in Table 1 are the g tensors and the hfc tensors of the alkali metal and chlorine nuclei of the Na:HCl and K:HCl complexes determined earlier by Lindsay et al.^{2,3} It is clearly revealed that the SOMOs of these complexes and that of the Li:HCl complex are essentially identical. Also included in the table are the hfc constants of hydrogen and lithium atoms

isolated in argon matrixes. Thus, for the Li:HCl complex, the observed hydrogen coupling constant indicates the unpaired electron density of ~ 0.9 in the hydrogen 1s orbital. Based on the Hartree–Fock wave functions, the anisotropy of the hfc tensor, $A_{\parallel} - A_{\perp}$, for a unit spin density in the chlorine 3p orbital has been computed to be 188 G.¹¹ The anisotropy of the observed chlorine hfc tensor, 27 G, thus indicates an unpaired electron density of ~ 0.14 in the chlorine 3p orbital. It must be concluded that, in the SOMO given by the AM1 method (eq 1), the unpaired electron density in the hydrogen orbital is underestimated while that in the chlorine orbital is overestimated. Similarly, for the Li:HF complex, the observed Li hfc tensor indicates the unpaired electron density of 0.63 in variance with a much larger value given by the AM1 theory (eq 2). It is surmised that the theory underestimates the degree of the sp hybridization. In the case of the Li:LiCl complex, the observed Li hfc tensor indicates the unpaired electron density of 0.32 in each of the Li 2s orbitals in a reasonable agreement with the SOMO given by the AM1 method (eq 3).

Some nontrivial discrepancies in the computed unpaired electron distributions in the final product radicals notwithstanding, the present study has clearly demonstrated the power and efficacy of the semiempirical SCF molecular orbital method (such as AM1) in elucidating the reaction process between an alkali metal atom and a hydrogen halide molecule and the structure and the electronic state of the final adduct radical. The reaction is driven by the three electron bonding scheme given by the unpaired electron of the alkali atom in its valence orbital

and the pair of electrons in the halogen p_{π} orbital. Two of the electrons move into the orbital given by the bonding combination of the two orbitals, and the third electron moves into the orbital given by the antibonding combination; if and when the latter orbital level crosses the antibonding σ orbital of the H–X sector, the migration of the unpaired electron into that sector occurs. A completely analogous reaction was found to occur between a Li atom and a LiCl molecule. The reaction processes of these systems and several others elucidated by semiempirical SCF methods may be viewed on the Web page www.almaden.ibm.com/st/people/kasai.

References and Notes

- (1) Kasai, P. H. *J. Am. Chem. Soc.* **1998**, *120*, 7884.
- (2) Davies, M. A.; Lindsay, D. M. *Surf. Sci.* **1985**, *156*, 335.
- (3) Lindsay, D. M.; Symons, M. C. R.; Herschbach, D. R.; Kviram, A. L. *J. Phys. Chem.* **1982**, *86*, 3789.
- (4) Dewar, M. J. S.; Zoebisch, E. G.; Healy, E. F.; Stewart, J. J. P. *J. Am. Chem. Soc.* **1985**, *107*, 3902.
- (5) Kasai, P. H. *Acc. Chem. Res.* **1971**, *4*, 329.
- (6) Kasai, P. H.; Whipple, E. B.; Weltner, W., Jr. *J. Chem. Phys.* **1966**, *44*, 2581.
- (7) *HyperChem*, release 5; Hypercube, Inc.: Gainesville, FL, 1996.
- (8) See, for examples, the following and the references therein: (a) Chen, M. L.; Schaefer, H. F., III. *J. Chem. Phys.* **1980**, *72*, 4376. (b) Aguado, A.; Paniagua, M.; Lara, M.; Roncero, O. *J. Chem. Phys.* **1997**, *107*, 10085.
- (9) Kasai, P. H. *J. Am. Chem. Soc.* **1972**, *94*, 5950.
- (10) Each A_{ij} was evaluated numerically (a summation over a given volume), and the orientation was determined from the similarity transformation necessary for the diagonalization of the resulting tensor.
- (11) Morton, J. R.; Preston, K. F. *J. Magn. Reson.* **1978**, *30*, 577.